5-12-2018

Review of solid polarized targets

Leiqaa Kurbany
University of New Hampshire, Durham

Review of Solid Polarized Targets

By Leiqaa Kurbany

Director, Karl Slifer Associate Professor of Phyiscs

University of New Hampshire

MAY 2018

1 Review of Solid Polarized Targets

ABSTRUCT

In the following pages I review polarized solid-state target briefly. What I discovered through my reading and writing about this technology, that is amazing tool to study the nucleon structure. I started with what is polarized solid-state target, went through Dynamic Nuclear Polarization (DNP) to understanding how it works, then its setup, in what experiments they used polarized solid-state target and some results of these experiments and finally I wrote a brief definition to many of terms, they are important to know to understand what is polarized solid state target.

1.Introduction:

The polarized solid-state target is an indispensable tool in numerous nuclear and particle physics experiments with high energy electrons, muons, and neutrinos, which have been used to characterize the parton substructure of the nucleon and to establish the current theory of the strong interaction, quantum chromodynamics (QCD). Scattering experiments such as the spin structure of the nucleon, the electromagnetic structure of the nucleon in its ground state, the structure of the nucleon excited states and the structure of light nuclei are employing polarized targets and beams give access to a number of physical observables of great interest which are measurable only by utilizing spin degrees of freedom[1]. The availability of the polarized proton and, then, deuteron (neutron) targets, proton polarizations near 100% and deuteron polarizations higher than 50% have been achieved in various materials, whose spin could be oriented in any direction, allowed the detailed study of hadron hadron interactions. In interactions with spinless particles, such as π and K-mesons, the spin-sensitive part could be extracted and used to discriminate among various theories. Together with polarized nucleon beams it became possible to study extensively the nucleon-nucleon interaction [2]. Meanwhile there was less progress using polarized targets with electrons, due to limitations in technology and the limited gain in understanding of the underlying physics processes that polarizing only the nucleon could provide. But the big question is why experiments in electron-nucleus scattering made use of polarized nuclei and polarized electron beams employing polarized targets have acquired increased importance? The first reason is in the past, only a small subset of experiments in electron-nucleus scattering made use of polarized nuclei and polarized electron beams. This was due to both the limitations in target technology, and the difficulties of producing polarized electron beams. The production of polarized electron beams recently has made great progress, with the use of stressed GaAs photocathodes, which have made possible the production of beams of polarization exceeding 80% with high intensities and good reliability. In addition, significant progress has been made in measuring accurately the polarization of the high-energy electrons. With these developments some of the necessary preconditions for the measurement of precise polarization observables are fullfed.

The second reason is the developments of the past few years which, today, allow the operation of electron accelerators with polarized continuous beams. With the increase in duty cycle by a factor 100-10000, coincidence experiments have become much more practical. Coincidence experiments provide much more detailed information than the inclusive (e,e`) experiments that up till now were the standard[3].

Quantum chromodynamics (QCD) has led to a theoretical description of the strong interaction in terms of the fundamental constituents, quarks and gluons. In the high-energy limit the internal structure of the nucleon can be well described by perturbative quantum chromodynamics (pQCD) due to the weak coupling in this energy regime. Deep inelastic lepton-nucleon scattering, together with the e^+e^- collision experiments, is well established as a powerful tool for the investigation of nucleon structure. The measured structure functions have been successfully interpreted in terms of parton distributions showing that quarks and QCD are on firm footing. The Standard Model tells that the valence quarks and the sea quarks are spin-1/2 objects bound by gluons which are spin-l objects. The presence of constituents with spin inside the hadrons has moved the question of spin phenomena to the forefront of high energy physics experiments [4]. A full understanding of how spin-1/2 quarks and spin-1 gluons play one's part to give nucleons a spin of-1/2 cannot be far off with polarized target technologies because trailing close behind the unpolarized deep inelastic scattering (DIS) experiments has been a polarized DIS program aimed at studying the spin structure of the nucleon using polarized lepton beams (electrons and muons), Leptons provide a wonderfully clean probe of the nucleon's substructure, since they only interact with quarks via the electromagnetic interaction and are transparent to strong interactions within the nucleon, scattered by polarized targets. These fixed-target experiments have been used to characterize the spin structure of the proton and neutron and to test additional fundamental QCD and quark-parton model (QPM) sum rules. The first experiments in polarized electron–polarized proton scattering, performed in the 1970s, helped establish the parton structure of the proton. In the late 1980s, a polarized muon–polarized proton experiment found that a QPM sum rule was violated, which seemed to indicate that the quarks do not account for the spin of the proton. This "proton-spin crisis" gave birth to a new generation of experiments at several high-energy physics laboratories around the world. The new and extensive data sample collected from these fixed-target experiments has enabled a careful characterization of the spin-dependent parton substructure of the nucleon [1]. To address a special problem by scattering experiments, first of all the given (polarized) beam characteristics e.g. stored beam, external beam, beam intensity etc. are decisive for the choice of the target type. Triggered by the many technical developments in different fields over more than four decades a variety of highly functional polarized target systems has been developed. Solid H and D targets, internal gaseous H, D and 3He targets, gaseous 3He are common polarized targets are used. Each of these target types has its own combination of highly sophisticated techniques, which result in specific advantages for the polarization experiments such as high nuclear polarization, high density, high purity of polarizable target material and reasonable polarization resistance during the experiments. All the manifold developments have made it possible to access progressively lower cross section interactions with better precision [4].

2. Dynamic Nuclear Polarization

Dynamic Nuclear Polarization (DNP) is a phenomenon by which high spin polarization, typically derived from a bath of free radical electrons, is transferred to a nuclear spin bath, enhancing the difference between the nuclear energy levels and thereby producing dramatically enhanced NMR signals for detection. The phenomenon was first predicted by Overhauser, but was not observed experimentally until the work of Slichter in metals in 1953.It was soon understood that the same technique could be used to develop high polarizations of 1H, 2H, and 13C in non-conducting solids. This advance became foundational for production of solid targets for high energy physics research.

2.1 Definition Of DNP

The general definition of Dynamic Nuclear Polarization can give by considering a solid sample containing host nuclei with nuclear spins I and paramagnetic impurities with electron spins

S. Spin polarization $P_{I,s} =< I^{Z}, S^{Z} > /(I, S)$ is defined as a fraction of spins (nuclear or electronic) directed along the external magnetic field ***H***|| ***f***or spins 1⁄ 2, the polarization values at the equilibrium temperature T_0 are

$$P_{I,S}^{0} = \tanh(\frac{\hbar\gamma_{I,S}H}{2K_B T_0}) \quad (1)$$

where $\gamma_{I,S}$ are the nuclear and electronic magnetogram ratios, respectively, One can see that, even at high magnetic field of 5 T and very low temperature T_0 = 0.5 K, the equilibrium polarization of protons is merely about 0.01, whereas $P_S^0 \approx -1$[5].

2.2 The DNP methods:

Since 1962 a variety of polarized target systems have been developed to reach high values of nuclear polarization by various methods. However, there are two major steps, which are common to all of them. The first step always consists of producing an atomic polarization in the sample. Because the electron magnetic moment exceeds that of the nucleus by a huge factor the polarization of an electron system is much easier to achieve than polarizing the nuclear spin system directly. In the second step the hyperfine interaction between the atomic spin *J* and the nuclear spin *I* is exploited to transfer the atomic polarization to the nucleus [4].

The mechanisms for DNP can be subdivided into two families. In one family, known as the solid effect, the polarization transfer is achieved in a single step. The microwave field combines with the super-hyperfine interaction to induce so-called forbidden transitions, simultaneous flip-flop or flip-flip transitions of an electron spin and a nuclear spin [6],

$$|m_s, m_I\rangle = \left|+\frac{1}{2}, -\frac{1}{2}\right\rangle \leftrightarrow \left|-\frac{1}{2}, +\frac{1}{2}\right\rangle \quad (2)$$

$$|m_s, m_I\rangle = \left|+\frac{1}{2}, +\frac{1}{2}\right\rangle \leftrightarrow \left|-\frac{1}{2}, -\frac{1}{2}\right\rangle \quad (3)$$

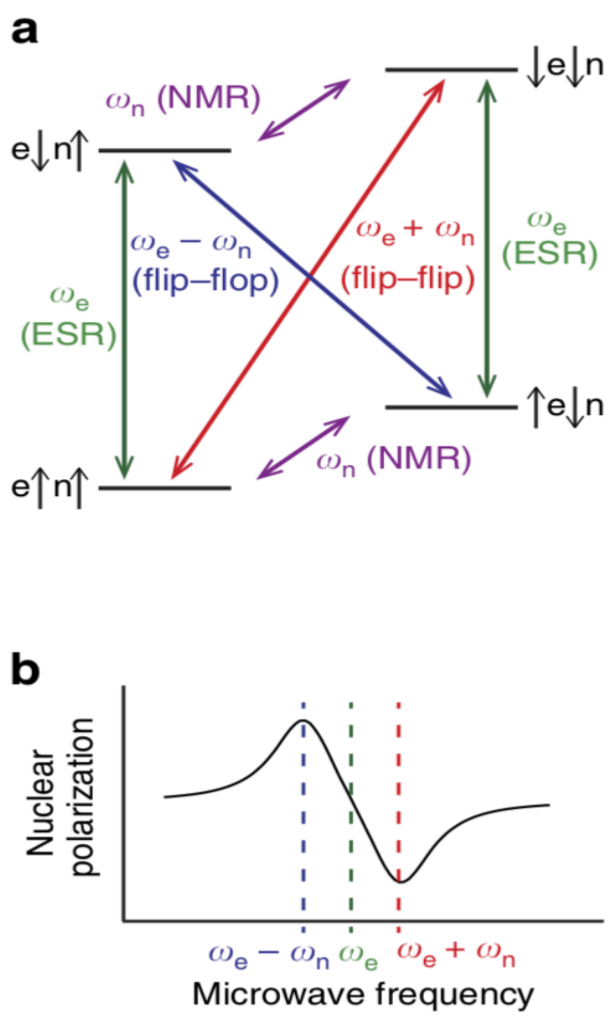

Figure 1: Energy level diagram for a dipolar-coupled electron spin-1/2 (e) and a nuclear spin-1/2 (n) system in a magnetic field. The ESR at frequency ω_e (green), NMR at frequency ω_n (purple), flip–flop at frequency $\omega_e - \omega_n$ (blue), and flip–flip at frequency $\omega_e + \omega_n$ (red) transitions are shown. Driven flip–flop transitions involve a mutual electron flip and a nuclear flop resulting in a positive nuclear polarization. Driven flip–flip transitions result in a negative nuclear polarization. (b) Schematic showing positive and negative nuclear polarization when driving flip–flop and flip–flip transitions, respectively[7].

In the other family, to be denoted as thermal mixing, the transfer occurs in a two-step process. First, the microwave field flips electron spins in normal ESR transitions. Next, the super-hyperfine interaction and the mutual interaction between the electron spins combine to induce triple spin flips, in which two electron spins and a nuclear spin flip simultaneously [6]:

$$|m_s, m_s', m_I\rangle = \left|+\frac{1}{2}, -\frac{1}{2}, -\frac{1}{2}\right\rangle \leftrightarrow \left|-\frac{1}{2}, +\frac{1}{2}, +\frac{1}{2}\right\rangle \quad (4)$$

$$|m_s, m_s', m_I\rangle = \left|+\frac{1}{2}, -\frac{1}{2}, +\frac{1}{2}\right\rangle \leftrightarrow \left|-\frac{1}{2}, +\frac{1}{2}, -\frac{1}{2}\right\rangle \quad (5)$$

Also, these triple spin flips transfer the polarization from one of the two electron spins to the nuclear spins.

2.3 The Solid Effect

A very simplified description of the solid-state effect can be given as follows: A suitable solid target material with a high concentration of polarizable nucleons is doped with paramagnetic radicals which provide unpaired electron spins [2].

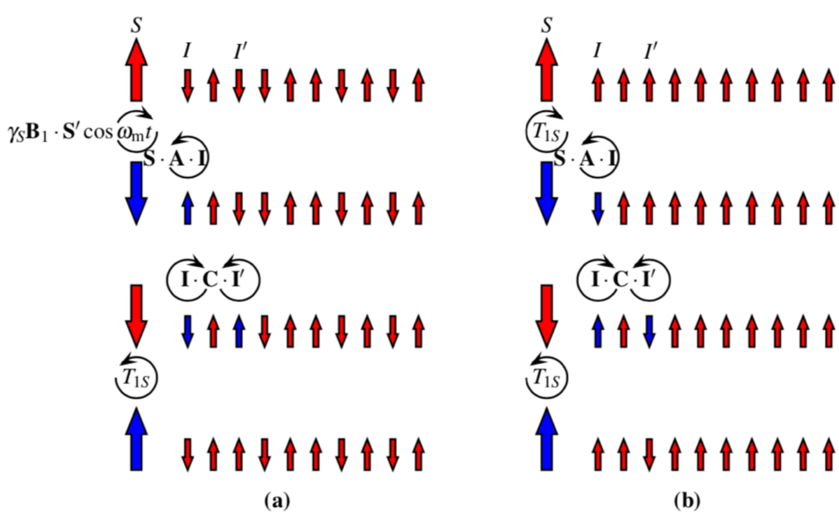

Figure 2:(a) Cartoon depicting the fundamental processes involved in DNP via the solid effect.

(b)Cartoon depicting the fundamental processes involved in direct nuclear spin-lattice relaxation ([6]*).*

A simple picture of the various processes playing a role in the solid effect is provided in Figure 2a. The big arrow represents an electron spin S and the small arrows some surrounding nuclear spins *I, I′*, etc. The direction of the arrows corresponds to the polarization of the spins. The top row shows the initial conditions. We start with a high electron spin polarization P_S, so the big arrow points up, while the nuclear spin polarization P_I is still low, so the small arrows are oriented randomly.

The aim of DNP is to polarize all nuclear spins, i.e., to point all small arrows in the same direction. To point them all up, the microwave frequency ω_m is tuned to the difference $\omega_S - \omega_I$ of the resonance frequencies of the electron spin S and a nearby nuclear spin I. Then the super-hyperfine interaction $\boldsymbol{S} \cdot \boldsymbol{A} \cdot \boldsymbol{I}$ and the microwave field cooperate to flip these two spins simultaneously. Such combined spin flips are known in the literature as forbidden transitions, though it would be more appropriate to denote them as second order transitions. As seen in the second row, the polarization of the electron spin is transferred to the nearby nuclear spin. Subsequently the resulting nuclear spin polarization needs to be transported to the nuclear spins further away. The third-row shows, how flip-flop transitions

$$|m_s, m_I\rangle = \left|+\frac{1}{2}, -\frac{1}{2}\right\rangle \leftrightarrow \left|-\frac{1}{2}, +\frac{1}{2}\right\rangle \tag{2}$$

Induced by the mutual interaction $I \cdot C \cdot I'$ between the nuclear spins take care of this transport. This process is known as *nuclear spin diffusion*. Finally, the electron spin *S* flips back via electron spin-lattice relaxation, so the whole process can start all over again and more nuclear spins can be polarized.

The fundamental process of the solid effect is the simultaneous transition of an electron spin and a nuclear spin leading from the first to the second row. This transition needs to conserve energy. So, the matching condition $\omega_s = \omega_m \pm \omega_I$ must hold in order to transfer polarization from the electron spins to the nuclear spins [6].

2.3.1 The Varieties of The Solid Effect.

1- The *well- resolved solid effect*. It occurs when the ESR spectrum is narrow, and the width is smaller than the resonance frequency ω_{0I} of the nuclear spins. Then, for some microwave frequencies the matching condition can hold with the + sign and for some other microwave frequencies with − sign. But the matching condition can never hold with the + sign and the − sign simultaneously. So, either only positive polarization is transferred, or only negative polarization [6].

2- The *differential solid effect*. This variety of the solid effect occurs when the ESR spectrum is broad, and their width is of the same order of magnitude as ω_{0I}. Then, for some microwave frequencies there may be electron spins obeying the matching condition with the + sign, as well as electron spins obeying the matching condition with the − sign. As a result, positive and negative polarizations are transferred simultaneously, and the net transfer is the difference between the two. Moreover, the microwave field also saturates electron spins with a resonance frequency $\omega_S \approx \omega_m$. If spectral diffusion is slow, the microwave field only burns a hole in the ESR signal and the electron spins obeying the matching condition $\omega_S = \omega_m \pm \omega_I$ are not affected [6],[7].

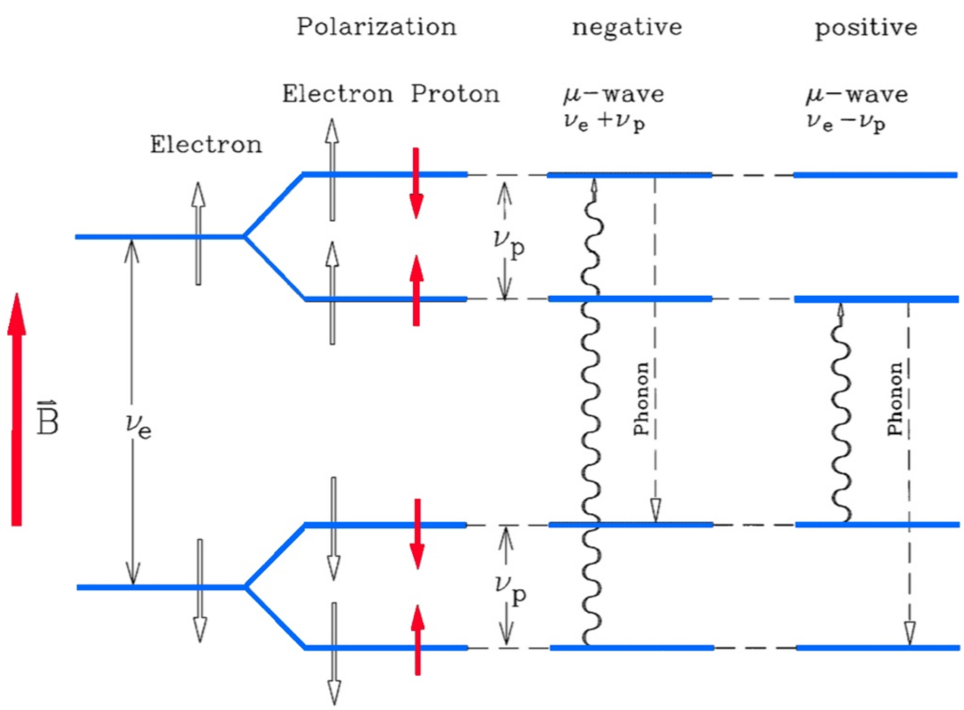

Figure 3: Schematic demonstration of the resolved solid-state effect [2].

2.4 Nuclear Spin- Lattice Relaxation

It would be great, if after DNP all nuclear spins were to stay polarized forever, so we could use these polarized spins all the time required by our applications. But the very electron spins, that we need to polarize the nuclear spins with DNP, also destroy the nuclear spin polarizations by means of nuclear spin-lattice relaxation. There are two channels through which this nuclear spin-lattice relaxation can take place:

1- *Direct nuclear spin-lattice relaxation:* - it is related to the solid effect and the electron spin-lattice interaction flips the big arrow between up and down with the electron spin-lattice relaxation rate T_{1S}^{-1}. Every once in a while, the electron spin-lattice interaction combines with the super-hyperfine interaction $S \cdot A \cdot I$ and flips both an electron spin and a nearby nuclear spin. Transfers the polarizations from this nearby nuclear spin back to the electron spin. Subsequently the mutual interaction $I \cdot C \cdot I^{'}$ between the nuclear spins induces flip-flop transitions, spreading this loss of polarizations to the nuclear spins further away. As the electron spin continues flipping up and down through electron spin-lattice relaxation, the process is repeated again and again, until all the nuclear spin polarizations are lost.

2- *Indirect nuclear spin-lattice relaxation*: - it occurs via mechanism of thermal mixing of Nuclear Polarization.

2.5 Thermal Mixing

Thermal mixing has proven itself most powerful for the orientation of nuclear spins in polarized targets and hyperpolarization for magnetic resonance imaging (MRI) [8]. The mechanisms put to work are the following. Microwave irradiation close to the electronic resonance frequency produces a change of the non-Zeeman electronic energy: towards lower or higher energy when the irradiation frequency is below or above the electronic Larmor frequency, respectively. Through thermal mixing the electronic non-Zeeman reservoir is in close thermal contact with the nuclear Zeeman reservoir and their common spin temperature evolves towards a positive or negative value when the irradiation frequency is below or above the electronic Larmor frequency, respectively. The system is then characterized by two temperatures, one for the electronic term and one for the combined electronic non-Zeeman plus nuclear Zeeman terms. All parts of the system are furthermore coupled to the lattice and experience relaxation. The heat capacity of the nuclear Zeeman term being much larger than that of the electronic non-Zeeman term, because of the high dilution of electronic spins, the relaxation time of the combined electronic non-Zeeman plus nuclear Zeeman reservoir is much longer than that of the electronic Zeeman reservoir, T_{1e}. The balance between the different mechanisms determines both the rate and the steady state of the dynamic nuclear polarization. This is schematically depicted in Fig. 4[9].

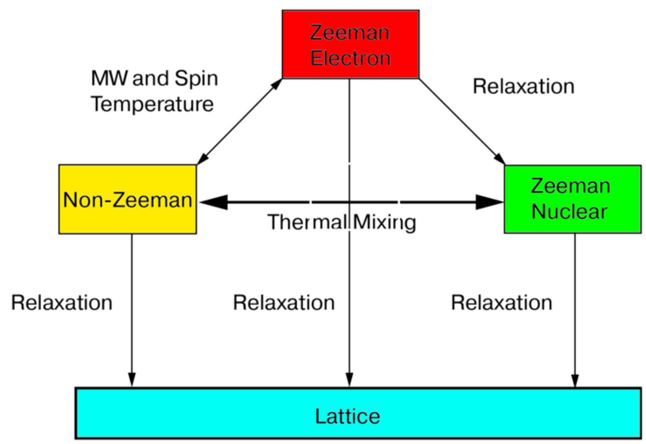

Figure 4: Block diagram of thermal couplings between four thermal reservoirs: electronic Zeeman, electronic non-Zeeman, nuclear Zeeman and lattice, in the course of DNP under microwave irradiation [9].

A simple picture of the processes playing a role in DNP via thermal mixing is presented in Figure 5a. The large arrows represent the polarization of several electron spins S, S', etc., and the small arrows the polarization of some nuclear spins I, I', etc., surrounding S. The top row shows the initial conditions. As in our description of the solid effect we start with a high electron spin polarization, and a low nuclear spin polarization. So, as in Figure 5a all large arrows are up, and the orientation of the small arrows is random. Again, our aim is to render all small arrows up. But to achieve this aim, we now tune the microwave frequency to the resonance frequency ω_s of the electron spin S''. As a result, this electron spin flips and we arrive at the situation depicted in the second row. The mutual interaction between the electron spins induces flip-flop transitions and the reversal of the polarization of S'' is rapidly transferred to another spin, e.g., S'. But once in a while, the mutual interaction $\boldsymbol{S'} \cdot \boldsymbol{D} \cdot \boldsymbol{S}$ between, e.g., S' and S combines with the super-hyperfine interaction $\boldsymbol{S \cdot A \cdot I}$ and induces a *triple spin flip* of the two electron spins and a nearby nuclear spin I. The rate of such triple spin flips is much smaller than the rate of simple flip-flop transitions.

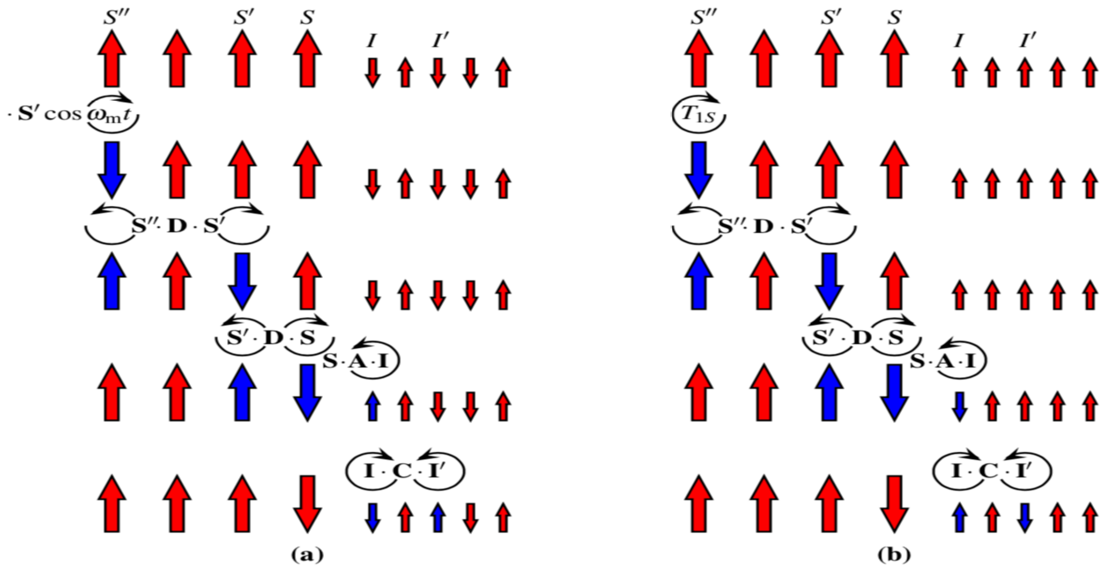

Figure 5: (a) Cartoon depicting the fundamental processes involved in DNP via thermal mixing. (b) Cartoon depicting the fundamental processes involved in nuclear spin-lattice relaxation via thermal mixing.

Simple flip-flop transitions may occur before a triple spin flip takes place. The third row shows how triple spin flips transfer the polarization of S to a nearby nuclear spin, while S' recovers its original orientation.

Subsequently, just as in the solid effect the resulting nuclear spin polarization is transported to the nuclear spins further away by the mutual interaction $\boldsymbol{I \cdot C \cdot I'}$ between the nuclear spins. Furthermore, the electron spin S flips back via electron spin-lattice relaxation or a flip-flop transition with another electron spin. This allows the process to start all over again, so more nuclear spins are polarized. But this last step is omitted from the figure. Triple spin flips as shown in Figure 5a not only serve to increase the nuclear polarization when a microwave field is applied. They also contribute to nuclear spin-lattice relaxation in a mechanism, of *indirect nuclear spin-lattice relaxation*[6].

3. Polarized target systems

Dynamic nuclear polarization (DNP) is a standard technique for producing polarized solid targets for nuclear and particle experiments. To realize DNP, a paramagnetic species in the form of a free or unpaired electron is introduced into the target material, either by dissolving a stable radical into the material (if the latter is liquid at room temperature), or by producing radicals directly within the material using ionizing radiation. The electrons are highly polarized by cooling the sample to a low temperature and exposing it to a high magnetic field. For example, at the 1 K and 5 T operating conditions of this target, the electron polarization is 99.8%. Off-center microwave saturation of the radicals' Electron Spin Resonance (ESR) frequency is then used to transfer their polarization to nearby nuclei, with one or more mechanisms, such as the solid effect, thermal mixing, being responsible for the polarization transfer .The polarization of nuclei near the paramagnetic radicals is transported throughout the bulk of the sample via spin diffusion, and may be positive or negative, depending upon whether the microwave frequency is below or above the ESR frequency. In well-designed systems, proton polarizations exceeding 95% have been achieved [10].

The general setup of the target system is shown in Fig. 6. The main component are;

- The superconducting split coil system because the nuclear spins in the solid targets are polarized with dynamic nuclear polarization method typically in 2.5 or 5 T magnetic field.
- The evaporation refrigerator which cools the target.
- The microwaves which induce spin flip transitions in the target because during the polarization build up a microwave generator pumps the paramagnetic centers in the target material close to the electron spin resonance frequency (about 70 GHz in 2.5 T field).
- The NMR system needed to measure accurately the target polarization.
- The target itself, the properties of a good polarized target material are high number of polarizable nucleons compared to the total amount of nucleons, high polarization degree, short polarization build up time, slow polarization loss rate in frozen spin mode, good resistance against radiation damage and easy handling of the target material. Commonly used target materials are butanol and ammonia [10],[11].

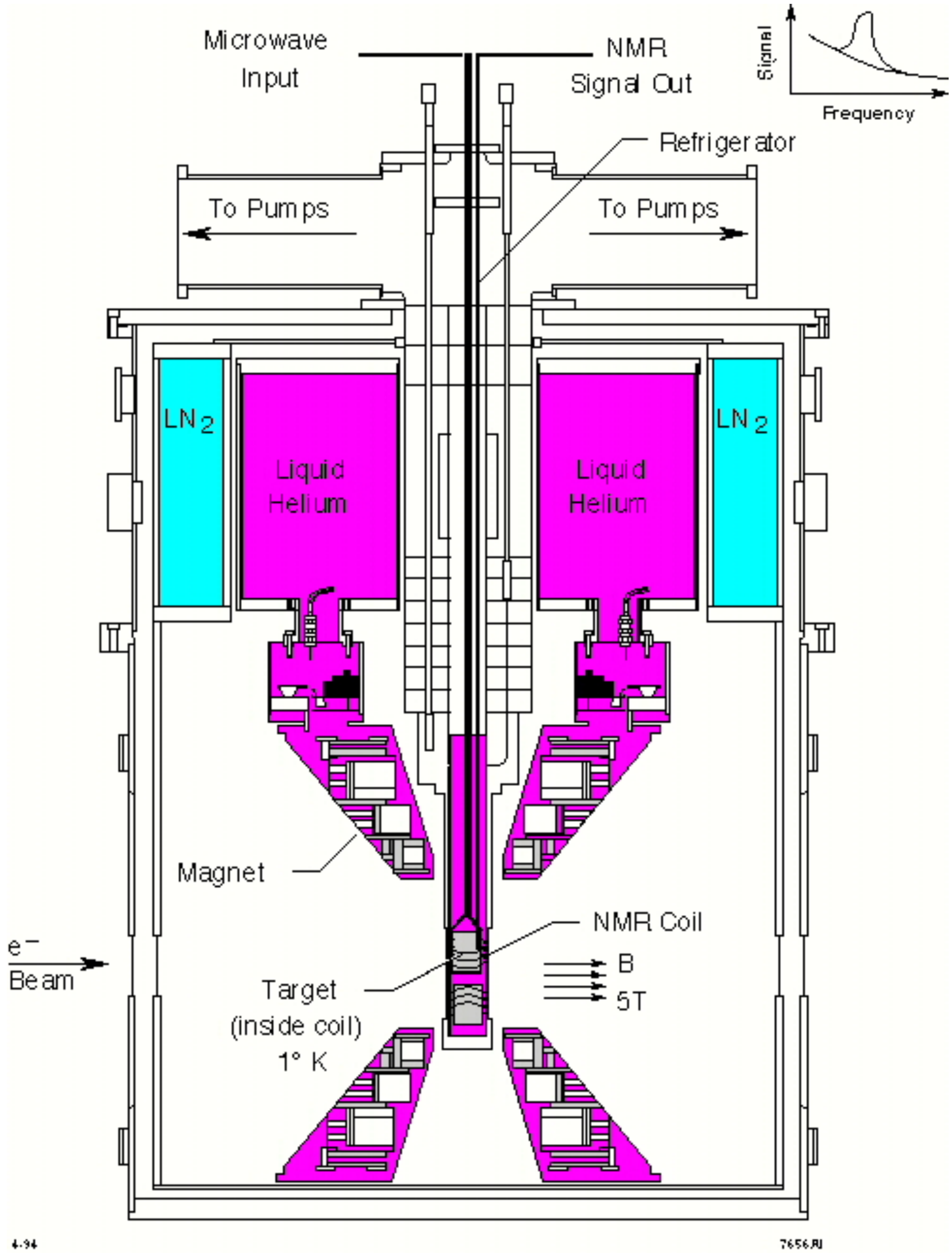

Figure 6: A generic polarized target showing the major subsystems and typical operational parameters.

4. POLARIZED TARGET EXPERIMENTS: -

Many modern experiments in nuclear and particle physics benefit from the exploitation of polarized targets and polarized beams these experiments include: -

- *The spin structure of the nucleon*: The internal structure of the nucleon in terms of the elementary constituents, the quarks and gluons, depends on the spins and angular momenta of these constituents. These contributions can be measured in deep inelastic scattering (DIS) of polarized leptons from polarized protons and neutrons[3].
  One of the review papers to study the spin structure of the nucleon conducted by S.E. Kuhn, J.-P. Chen, E. Leader and others, they focused in particular on the spin structure functions g_1 and g_2 of the nucleon and their moments. Their data, in combination with the earlier ones, allow them to study in detail the polarized parton densities, the Q^2 dependence of various moments of spin structure functions, the duality between deep inelastic and resonance data, and the nucleon structure in the valence quark region. In their published in 2009, they put limits on the flavor decomposition and the gluon contribution to the nucleon spin [12].

- *The electromagnetic structure of the nucleon in its ground state*: The magnetic and electric form factors of the nucleon give detailed information on the distribution of the constituents in coordinate space, and a separation of the electric and magnetic form factors, which contribute incoherently to the unpolarized cross section, is possible when using polarized nucleons. Without polarized targets and/or beams, only the dominating form factor at larger momentum transfers this is the magnetic one can be measured with satisfactory accuracy[3].

  John Arrington, Kees de Jager and Charles F. Perdrisat (2011) reviewed the spatial distribution of the proton charge and magnetization, providing the most direct connection to the spatial distribution of quarks inside the proton by measuring the form factors, because the charge and magnetization distributions of the proton and neutron are encoded in their elastic electromagnetic form factors, which can be measured in elastic electron–nucleon scattering[13].

Ryan Zielinski with the E08-027 collaboration (2017), measured the spin structure functions of the proton at Jefferson Laboratory in Newport News, Va. Longitudinally polarized electrons were scattered from a transversely and longitudinally polarized solid ammonia target in Jefferson Lab's Hall A, with the polarized NH_3 acting as an effective proton target. Focusing on small scattering angle events at the electron energies available at Jefferson Lab, his experiment covered a kinematic phase space of 0.02 $GeV^2 < Q^2 < 0.20$ GeV^2 in the proton's resonance region. The spin structure functions, $g_1^p(x, Q^2)$ and $g_2^p(x, Q^2)$ are extracted from an inclusive polarized cross section measurement of the electron-proton interaction [14].

- *The structure of the nucleon excited states*: At excitation energies of 1 GeV, the nucleon exhibits a number of broad, but identifiable excited states. The separation of these overlapping resonances from each other, and the measurement of the electric and magnetic transition form factors, is greatly facilitated by the use of polarized targets[3].
- *The structure of light nuclei*: As a consequence of the complicated dependence of the nucleon -nucleon force on spin and angular momentum, the wave functions of light nuclei (deuteron, He, He2) display a rich structure. Much of the interest today is centered on the smaller components involving angular momenta greater than zero, and these components can only be observed in measurements involving the spin observables accessible in experiments with polarized nuclei [2].The deuteron which is a spin 1 nuclear object, so there are three different helicity states; $m = \pm 1$, when the third component of the deuteron's spin is aligned or anti-aligned in the direction (z) of the incoming lepton, and $m = 0$, when the spin component along z is zero. As a result, the number of independent helicity amplitudes, hence the photo-absorption cross sections become 8 instead of 4. This requires four additional structure functions, usually referred to as b_{1-4}; These additional structure functions are called tensor structure functions, and all arise because of the binding effects between the proton and the neutron that form the deuteron [15].

5. Some Important Definitions

5.1 Deep Inelastic Lepton Scattering

The lowest order diagram for deep inelastic lepton scattering, $l + N \rightarrow l' + X$.

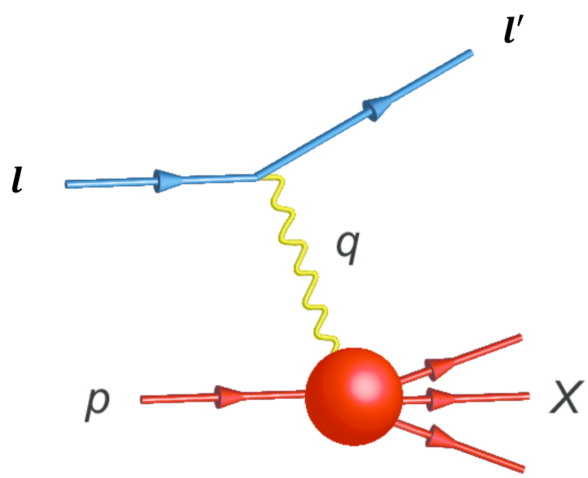

Figure 7: Schematic diagram of the Deep Inelastic Scattering (DIS) process.

Deep inelastic scattering (DIS) is the archetype for hard processes in QCD: a lepton — in practice an electron, muon or neutrino — with high energy scatters off a target hadron — in practice a nucleon or nucleus, transferring large quantities of both energy and invariant squared-four-momentum. For charged leptons the dominant reaction mechanism is electromagnetism and one photon exchange are a good approximation. For neutrinos either $W^{\pm}$ (charged current) or Z^{0} (neutral current) exchange may occur. Neutrino scattering experiments require far too massive targets for polarization to be a practical option, so we will ignore them, although W -exchange has been observed in $e^{-}p \rightarrow \nu_e + X$ and could be extended to a polarized target, at least in principle. Thus, we are mainly limited to charged lepton scattering by one photon exchange. The kinematics is shown in fig. (7). The initial lepton with momentum k and energy E exchanges a photon of momentum q with the target with momentum P. Only the outgoing electron with momentum k' and energy E' is detected. One can define the two invariants

$$q^2 \equiv (k-k')^2 = q_0{}^2 - \vec{q}^{\,2} = -4EE'\sin^2(\theta/2) = -Q^2 < 0 \tag{6}$$

$$\nu \equiv P \cdot q = M\,(E - E') \tag{7}$$

where; θ is scattering angle and $q^0 \equiv E - E'$ refers to the target rest frame.

The deep inelastic, or Bjorken limit is where Q^2 and ν both go to infinity with the ratio, $x \equiv Q^2/2\nu$ fixed. x is known as the Bjorken (scaling) variable. Since the invariant mass of the hadronic final state is larger than or equal to the mass of the target, $(P+q)^2 \geq M^2$, one has $0 < x \leq 1$. It is convenient also to measure the energy loss using a dimensionless variable,

$$0 \leq y \equiv \frac{\nu}{ME} \leq 1 \tag{8}$$

We will find E, Q^2, x, and y to be a useful set of variables. Note that it is overcomplete since $x\,y = Q^2/2ME$, and note also that what we define as ν differs from common usage by a factor of M. The behavior of cross sections at large Q^2 is much more transparent using these variables than using the set (E, E', θ) favored by experimenters for the reason that $\theta \to 0$ as $Q^2 \to \infty$ at fixed x and y [16].

5.2 The Cross Section for Polarized Scattering:

The differential cross section for unpolarized deep inelastic charged lepton scattering can be written, in the Born approximation,

$$\frac{d^2\sigma}{dQ^2dx} = \frac{4\pi\alpha^2}{Q^4}\frac{1}{x}\left[xy^2F_1(x,Q^2) + \left(1 - y - \frac{Mxy}{2E}\right)F_2(x,Q^2)\right] \tag{9}$$

where α is the electromagnetic coupling constant and $F\ (x, Q^2)$ and $F\ (x, Q^2)$ are the unpolarized structure functions of the nucleon. In the laboratory system, the polarized scattering process is conveniently visualized in the two planes depicted in Fig. 8. The scattering plane is defined by the momentum three-vectors $\vec{k}$ and $\vec{k}'$ of the incoming and scattered lepton, respectively. The spin plane is defined by $\vec{k}$ and by the spin vector $\vec{S}_N$ of the nucleon; β is the angle between $\vec{k}$ and $\vec{S}_N$ $(0 \leq \beta \leq \pi)$ and φ is the angle between the scattering and the spin planes.

The cross section for polarized scattering depends, in addition, on the relative orientation φ of the scattering and spin planes.

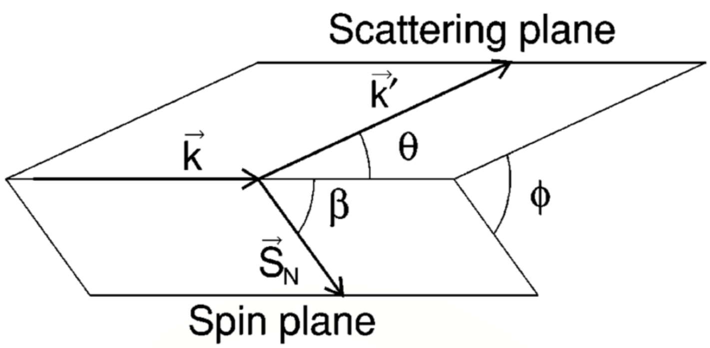

Figure 8: Scattering of longitudinally polarized leptons in the laboratory frame

This cross section can be decomposed into an unpolarized piece σ_0 and a polarized piece σ

$$\frac{d^3\sigma(\beta)}{dQ^2\,dx\,d\phi} = \frac{d^3\sigma_0}{dQ^2\,dx\,d\phi} - \frac{d^3\Delta\sigma(\beta)}{dQ^2\,dx\,d\phi} \tag{10}$$

where $d^3\sigma\,/dx\,dy\,d\varphi$ is the unpolarized cross section of Equation (9).

$$\begin{aligned}\frac{d^3\Delta\sigma(\beta)}{dQ^2\,dx\,d\phi} = \frac{4\alpha^2}{Q^4} y \Bigg\{ \cos\beta \left[\left(1 - \frac{y}{2} - \frac{\gamma^2 y^2}{4}\right) g_1(x, Q^2) - \frac{\gamma^2 y}{4} g_2(x, Q^2) \right] \\ - \cos\phi \sin\beta \frac{\sqrt{Q^2}}{\nu} \left(1 - y - \frac{\gamma^2 y^2}{4}\right)^{\frac{1}{2}} \\ \times \left[\frac{y}{2} g_1(x, Q^2) + g_2(x, Q^2) \right] \Bigg\},\end{aligned} \tag{11}$$

where $\gamma = \frac{2Mx}{\sqrt{Q^2}}$ and g_1, g_2 are the spin-dependent structure functions of the nucleon [1].

5.3 Structure Functions in Quark-Parton Model.

The spin-independent structure functions F_1 and F_2 have a straightforward interpretation in the QPM:

$$F_1(x) = \frac{1}{2}\sum_i e_i^2[q_i(x) + \bar{q}_i(x)], \tag{12}$$

$$F_2(x) = \sum_i e_i^2 x[q_i(x) + \bar{q}_i(x)]. \tag{13}$$

$$F_2(x) = 2xF_1(x). \tag{14}$$

In these expressions, $q_i(x)$ and $\bar{q}_i(x)$ are the densities of quarks and antiquarks, respectively; i is the quark flavor and e_i the quark electric charges.

The interpretation of the spin-dependent structure function g_1 is equally simple, and where $(q_i^+(x)\ (q_i^-(x))$ is the density of quarks of flavor i with helicity parallel (antiparallel) to the nucleon spin. This interpretation of $g_1(x)$ can be understood from the fact that a virtual photon with spin projection +1 can only be absorbed by a quark with spin projection −1/2, and vice versa.

The interpretation of the "*transverse*" spin structure function g_2 in the QPM is less obvious and has been the subject of much theoretical debate [1].

5.4 The Bjorken Sum Rule

It constitutes a very fundamental test of the structure or QCD, the polarized Bjorken sum rule refers to the integral over all x at fixed Q^2 of the difference between polarized structure functions of the proton g_1^p and the neutrong_1^n,

$$\Gamma^{p-n}(Q^2) = \int_0^1 g^p(x, Q^2) - g^n(x, Q^2)\, dx \tag{15}$$

The Bjorken integral can be written in terms of the QCD correction Δ_{Bj}

$$\Gamma_1^{p-n}(Q^2) = \frac{1}{6}\left|\frac{g_A}{g_V}\right|[1 - \nabla_{Bj}(Q_2)] \tag{16}$$

The value of the nucleon beta decay constant is taken to be $|g_A/g_V| = 1.2601 \pm 0.0025$ [17].

5.5 Tensor Structure Functions

The deuteron, a spin-1 target, has energy levels which split three ways in a magnetic field, $m = -1, 0, +1$. The target spin orientation can be described using the vector and tensor polarization. The tensor polarization, P_{zz}, can be expressed in terms of the vector polarization $P_{ZZ} = 2 - \sqrt{4 - 3P^2}$ [18].

The definition of vector polarization for spin-1 is

$$P = \frac{n_+ - n_-}{n_+ + n_- + n_0} = \frac{r^2 - 1}{r^2 + r + 1} \tag{17}$$

with the tensor polarization defined as

$$P_{zz} = \frac{n_+ - 2n_0 + n_-}{n_+ + n_- + n_0} = \frac{r^2 - 2r + 1}{r^2 + r + 1} \tag{18}$$

$where; \ r\ defined\ as\ r = I_+/I_-$

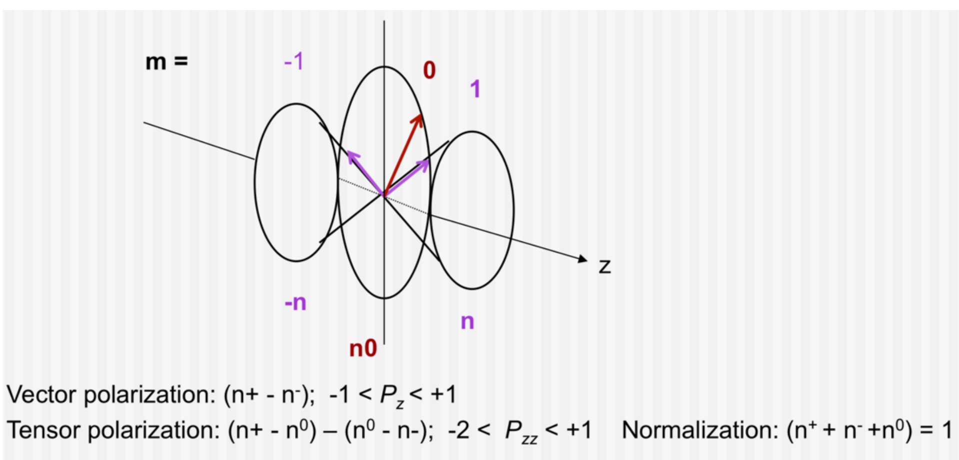

Figure 9: Spin-1 system in a B-field leads to 3 sublevels via Zeeman interaction

For a spin-one hadron such as the deuteron, there exist new polarized structure functions, b_1, b_2, b_3, and b_4, which could probe dynamical aspects including orbital motion within the hadron. The new structure is associated with tensor structure, so that the tensor-polarized structure functions vanish if constituents are in the S state. It is also important to investigate completely different spin quantities from the nucleon for establishing high-energy spin physics.

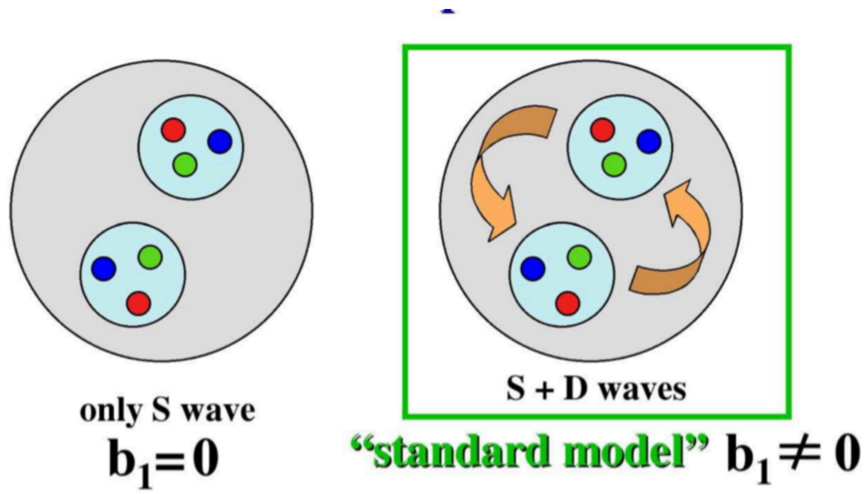

Figure 9. Tensor structure of the deuteron[18].

$$\frac{d^2\sigma}{d\Omega dE'} = \sigma_{Mott}\left[\frac{1}{v}F_2(x,Q^2) + \frac{2}{M}F_1(x,Q^2)tan^2\theta/2\right] + \gamma g_1(x,Q^2) + \delta g_2(x,Q^2) + \varsigma b_1(x,Q^2) + \varepsilon b_2(x,Q^2) + \xi b_3(x,Q^2) + \eta b_4(x,Q^2) \quad (19)$$

6. Summery

For the last four decades scientists and researchers have worked to improve solid polarized targets because they achieved a good explanation and results about the nucleons structure by using them in their experiments. These targets are on the steep rise, and new successes are expected in the near future. They are used to study the configuration of the spin on the nucleon and its structure for spin -1/2 nucleons by analysis spin structure functions and for spin-1 nucleons by analysis tensor structure functions.

Finally, a few words about the future. It seems that the steep rising of solid polarized targets development is far from its finish and the studies of spin and tensor-polarized structure functions could open a new era of high-energy spin physics.

7. Referances

[1] E. W. HUGHES and R. VOSS, “Spin structure functions,” *Annu. Rev. Nucl. Part. Sci.*, vol. 49, no. 1, pp. 303–339, Dec. 1999.

[2] D. G. Crabb and W. Meyer, “Solid polarized targets for nuclear and particle physics experiments,” *Annu. Rev. Nucl. Part. Sci.*, vol. 47, no. 1, pp. 67–109, Dec. 1997.

[3] T. D. Averett *et al.*, “A solid polarized target for high-luminosity experiments,” *Nucl. Instruments Methods Phys. Res. Sect. A Accel. Spectrometers, Detect. Assoc. Equip.*, vol. 427, no. 3, pp. 440–454, 1999.

[4] S. Goertz, W. Meyer, and G. Reicherz, “Polarized H, D and 3He targets for particle physics experiments,” *Prog. Part. Nucl. Phys.*, vol. 49, no. 2, pp. 403–489, Jan. 2002.

[5] V. A. Atsarkin, “Dynamic nuclear polarization: Yesterday, today, and tomorrow,” *J. Phys. Conf. Ser.*, vol. 324, no. 1, p. 012003, Oct. 2011.

[6] A. Abragam and M. Goldman, “Principles of dynamic nuclear polarisation,” *Reports Prog. Phys.*, vol. 41, no. 3, pp. 395–467, Mar. 1978.

[7] E. Rej, T. Gaebel, T. Boele, D. E. J. Waddington, and D. J. Reilly, “Hyperpolarized nanodiamond with long spin-relaxation times,” *Nat. Commun.*, vol. 6, no. 1, p. 8459, Dec. 2015.

[8] W. T. Wenckebach, “Dynamic nuclear polarization via thermal mixing: Beyond the high temperature approximation,” *J. Magn. Reson.*, vol. 277, pp. 68–78, Apr. 2017.

[9] M. Goldman, “Overview of Spin Temperature, Thermal Mixing and Dynamic Nuclear Polarization,” *Appl. Magn. Reson.*, vol. 34, no. 3–4, pp. 219–226, Aug. 2008.

[10] J. Pierce *et al.*, “Dynamically polarized target for the and experiments at Jefferson Lab,” *Nucl. Instruments Methods Phys. Res. Sect. A Accel. Spectrometers, Detect. Assoc. Equip.*, vol. 738, pp. 54–60, Feb. 2014.

[11] D. Keller, “Uncertainty minimization in NMR measurements of dynamic nuclear polarization of a proton target for nuclear physics experiments,” *Nucl. Instruments Methods Phys. Res. Sect. A Accel. Spectrometers, Detect. Assoc. Equip.*, vol. 728, pp. 133–144, Nov. 2013.

[12] S. E. Kuhn, J.-P. Chen, and E. Leader, “Spin Structure of the Nucleon -Status and Recent Results,” 2009.

[13] J. Arrington, K. de Jager, and C. F. Perdrisat, “Nucleon Form Factors - A Jefferson Lab Perspective,” Feb. 2011.

[14] R. Zielinski, “The g2p Experiment: A Measurement of the Proton’s Spin Structure Functions,” Aug. 2017.

[15] N. Guler *et al.*, “SPIN STRUCTURE OF THE DEUTERON,” 2009.

[16] R. L. Jaffe, “Spin, Twist and Hadron Structure in Deep Inelastic Processes,” Feb. 1996.

[17] K. A. Milton, I. L. Solovtsov, and O. P. Solovtsova, “The Bjorken Sum Rule in the Analytic Approach to Perturbative QCD,” Sep. 1998.

[18] S. Kumano, “Tensor-polarized structure functions: Tensor structure of deuteron in 2020’s,” Jul. 2014.